Comparison of combustion characteristics of magnesium and aluminum powders

R. Lomba , S. Bernard, P. Gillard and C. Mounaïm-Rousselle
PRISME - Université d'Orléans, 8 rue Léonard de Vinci 45072 Orléans, France
F. Halter , C. Chauveau
ICARE - CNRS, 1C avenue de la recherche scientifique 45071 Orléans, France
T. Tahtouh and O. Guézet
PSA Peugeot Citroën, 1 route de Gisy 78943 Vélizy-Villacoublay, France

1 Introduction

Metal particles are highly energetic materials, and their combustion is used in a variety of applications. In solid rocket motors (SRM), aluminum particles are used as an additive to increase the energy density and the specific impulse. A shift in the combustion mechanism for smaller aluminum particles has been the subject of several recent studies [1–3], mainly motivated by the faster reaction rates presented by smaller particles, which could shorten the necessary in-rocket residence time. Magnesium may also play a significant role in the next era of space exploration, as it is considered as a potential energy source for propulsion on lunar and Mars missions.

In addition, metal particles recently began to be considered as a potential energy carrier for terrestrial applications where high energy densities are required and for remote energy generation, with aluminum and magnesium being the most considered metals. Aluminum has a higher energy density and is more abundant on the earth's crust. On the other hand, magnesium is significantly easier to ignite and displays faster reaction rates. Both metals are also widely used in non-energetic applications, and knowledge of fundamental combustion characteristics is therefore necessary in order to mitigate dust explosion risks.

Comparing combustion characteristics for those metals is therefore of great practical interest. However, available data is still scarce, and most studies focused on isolated particles or low number density dust clouds. Recently, Santhanam et al. [4] have evaluated combustion characteristics of aluminum dust powders in constant volume explosions (CVE). In a previous work [5] , further investigation of the capabilities of standardized CVE experiments in retrieving combustion characteristics of aluminum dust flames has been conducted. The experiments were shown to be consistent with existing data and aluminum combustion trends. In the present work, combustion magnesium and aluminum powders in air was studied in a 20-l spherical bomb, and their measured combustion characteristics were compared.

2 Experimental setup

The aluminum powders used in this work are pure (> 99.8 %), spherical powders with Sauter mean diameters (d_{32}) varying between 7 μm and 18 μm, supplied by Poudres Hermillion. Magnesium powders

Correspondence to: ricardo.lombadearaujojunior@mpsa.com

are pure (> 99.8 %), irregularly shaped powders with $d_{32} = 38.3$ μm and a larger size distribution, supplied by Alfa Aesar. By sieving this powder, a magnesium powder sample with $d_{32} = 25.3$ μm was obtained. The size distributions were studied using a particle size analyzer, scanning electron microscopy (SEM) imaging and thermal gravimetric analysis (TGA). Parameters such as polydispersity, oxide layer thickness and mean representative diameter significantly influence dust powder combustion. It is therefore important to characterize the studied powders as much as possible. The powders were dried and sieved before each experiment in order to improve dispersion characteristics and break the largest particle agglomerates.

The explosion tests were run in a spherical 20-l explosion vessel, following the international standard EN 14034-3 (2006) with the exception of the ignition system. Prior to each test, the powder reservoir was loaded with a stoechimetric concentration of metallic powder and then pressurized to 12.0 bar, and the spherical vessel was partially vacuumed to 0.6 bar. Upon an external trigger, the electro-pneumatic valve separating the powder reservoir from the vessel is opened for 70 ms. Metal powder and synthetic air (Air Liquide, 80% O_2/ 20% N_2) enter the explosion vessel, and a rebound nozzle (Kuhner AG) disperses the aerosol throughout the chamber by generating a turbulent flow. At the end of the injection period, a target pressure of 1.0 bar is achieved. In order to reduce turbulence, a standard 60 ms delay is respected between injection and ignition. The aerosol is then ignited by an electric arc formed between two tungsten electrodes in the center of the sphere. Although no dust monitoring system was used during the experiments, the dispersion mechanism is well characterized in the literature. The turbulent flow field can be considered spatially homogeneous and directionally isotropic after 60 ms and thereafter [6]. Dust concentration was studied both experimentally and numerically [7, 8]. Although the numerically obtained dust concentration was typically lower than the nominal dust concentration, due to powder accumulation at the walls, a good dust homogeneity was observed.

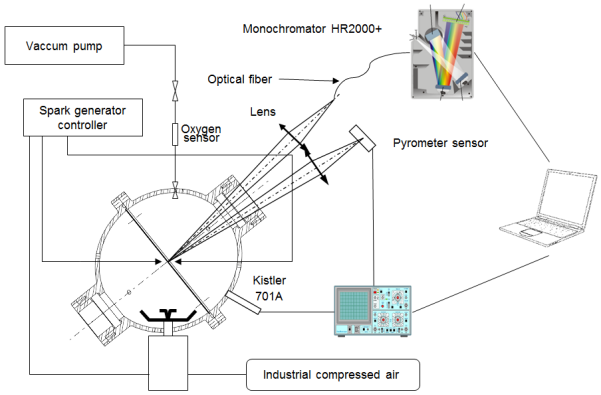

Figure 1: Schematic of the experimental setup

Data acquisition for flame propagation monitoring is composed by a pressure sensor (Kistler 701A, pressure range: $0-20$ bar), a custom IR bi-color pyrometer and a OceanOptics HR 2000+ spectrometer, placed behind an optical access. A set of lenses focuses light from the combustion experiment into the pyrometer and spectrometer. The combustion efficiency η_{comb} was estimated under the hypothesis that the only reaction taking place during combustion is 4 Al + 3 O_2 $\rightarrow$ 2 Al_2O_3 and 2 Mg + O_2 $\rightarrow$ 2 MgO. After the combustion event, the vessel was allowed to cool and a UEGO lambda sensor was connected to the internal gas phase and residual oxygen content, and thus a combustion efficiency, was measured. Figure 1 illustrates the combustion vessel along with the data acquisition equipment.

Flame temperatures were obtained with bi-color pyrometry from the continuous part of the flame spectra, and therefore correspond to the condensed-phase emitters temperature. The wavelength couples for deriving temperature were chosen to avoid the emission lines from gaseous species such as Al(g), Mg(g), AlO(g) and MgO(g). The temperature traces obtained are relatively stable during the pressure rise inside the vessel. Given that both the spectrometer and the bi-color pyrometer observe cumulative radiance through their line of sight, the estimated flame temperature was taken as the mean temperature value between the maximum rate of pressure rise and the maximum pressure inside the vessel, in order to minimize light emission/absorption from the unburned mixture.

Turbulent burning velocities were estimated assuming that, at any given time during an evaluation interval of the combustion event, the flame surface can be averaged and described by a sphere of an equivalent radius r_b, and that the combustion behavior is still governed locally by laminar processes. Under these assumptions, the flame propagation speed S_F can be defined as the derivative $S_F = dr_b/dt$. Taking into consideration the expansion of burned gases and disregarding the change in the number of moles and molecular mass of the gas, the turbulent burning velocity S_T can be written as $S_T = (\rho_b/\rho_u)S_F$, where ρ_b and ρ_u are, respectively, the mean density of the burned and unburned mixture. Using the expressions for adiabatic compression of the unburned mixture, it follows that [4, 9] :

$$S_T = \frac{dP}{dt}\frac{R}{3}\left(\frac{P_0}{P}\right)^{1/\gamma}\frac{1}{P_e - P_0}\left[1 - \left(\frac{P_0}{P}\right)^{1/\gamma}\frac{P_e - P}{P_e - P_0}\right]^{-2/3} \tag{1}$$

where P is the pressure inside the combustion vessel, dP/dt is rate of pressure rise, P_0 is the initial pressure, P_e is the maximum pressure achieved in the experiment, R is the vessel radius and $\gamma = 7/5$ is the heat capacity ratio of the gas.

Typical parameters used in CVE experiments to characterize explosion severity are the maximum pressure achieved P_e, reflecting the heat generated by the combustion; and the deflagration index K_{st}, reflecting the rate of pressure rise and thus the reaction rate, and is written as $K_{st} = \left(\frac{dP}{dt}\right)_{max} V^{1/3}$.

Silvestrini *et al.* [10] compiled a decent number of S_L^0 values for different dust-air mixtures and correlated with the K_{st} and P_e values from combustion tests run in a standardized 20-l spherical vessel, giving the semi-empirical correlation displayed in equation 2. The laminar burning velocity values obtained using this correlation are compared for the different powders studied in this work, as well as with existing laminar burning velocity values available in the literature.

$$S_L^0 = \frac{0.11\,K_{st}}{(P_e - P_0)}\left(\frac{P_0}{P_e}\right)^{0.14+1/\gamma} \tag{2}$$

3 Results

For each experimental test condition, at least two runs were performed, and the pressure traces obtained were considered to be repeatable. In figure 2a, the outer and inner border of the filled regions each represent an experiment itself, and thus the filled regions illustrate the repeatability of the experiment for each powder. Pressure traces from the same powder have similar values of P_e and similar slopes. Figure 2b represents the evolution of the rate of pressure rise during combustion for the same cases as figure 2a, which is directly correlated to the rate of reaction inside the vessel, and illustrates the significant influence of mean diameter on dust combustion.

Explosion severity was measured in terms of maximum pressure achieved P_e, reflecting the overall energy release, and the deflagration index K_{st}, reflecting the rate of pressure rise and thus the reaction rate. The induction period leading to a rapid pressure rise was defined, as in [4] , as the time from the beginning of the arc discharge to the time when a pressure rise of 10% of P_e was observed, representing the ignition delay of the aerosol.

In table 1, finer powders are shown to burn faster and more efficiently, evidencing a large influence of mean particle diameter on dust combustion. Magnesium powder is shown to burn faster than aluminum particles at equivalent diameter.

Laminar burning velocity values obtained with the correlation proposed by Silvestrini *et al.* [10] agreed well with the existing data [11–16], even though not much is known about metal burning velocities and

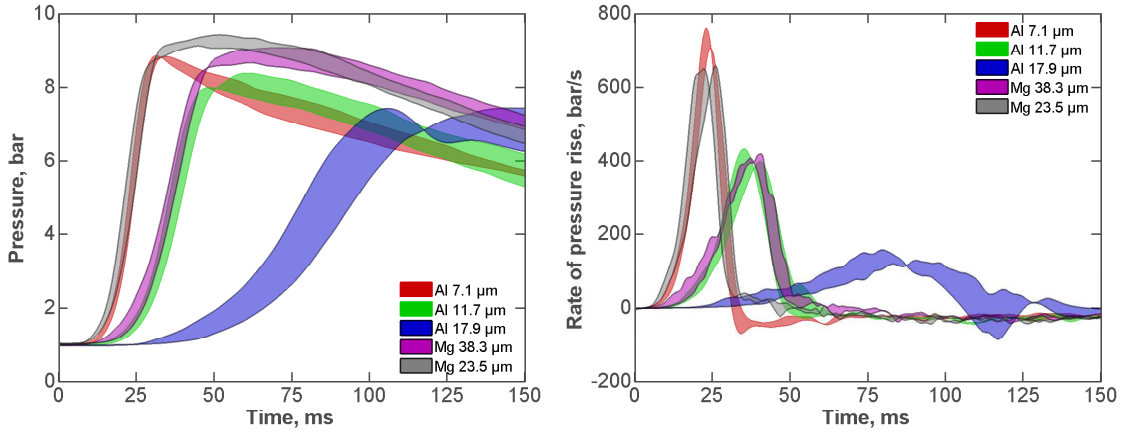

(a) (b)

Figure 2: Temporal evolution of (a) pressure and (b) rate of pressure rise inside the combustion vessel for different metallic powders.

Table 1: Summary of dust combustion characteristics

	Al 7.1 μm	Al 11.7 μm	Al 17.9 μm	Mg 23.5 μm	Mg 38.3 μm
η_{comb}	0.58	0.64	0.51	0.78	0.75
S_T, m/s	1.80	1.22	0.45	1.78	1.16

data scatter is still significant, as shown in figure 3a. Aluminum flame temperatures were observed to decrease with mean particle diameter, indicating a higher relative rate of heat loss and that the flame could have approached the particle surface. This tendency had previously been observed for isolated particles and low number density clouds burning in shock tubes, as illustrated in figure 3b.

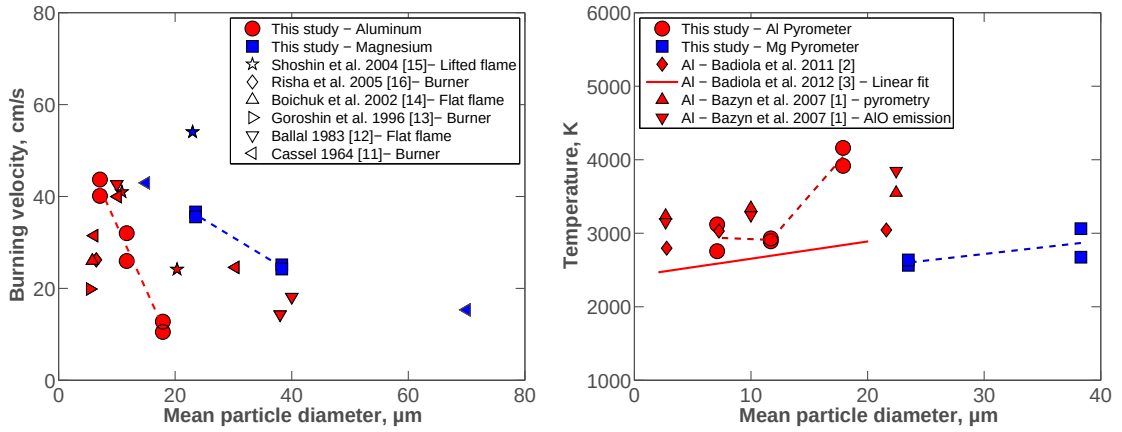

(a) (b)

Figure 3: Comparison between burning velocity and temperature measurements for aluminum (red) and magnesium (blue) powders obtained from CVE experiments and previous reported values in the literature. The dashed lines represent the mean values for the experiments presented in this study.

4 Discussions

One important phenomenon in describing metal particle combustion is the presence or not of vapor-phase reaction. In order to quantify the presence of vapor-phase species, the emission originating from the condensed-phase combustion products was simulated using a non-gray body emitter equation and optimizing a general scaling parameter and a condensed-phase temperature to fit the non-gray body spectrum to the experimental spectrum. The experimental emission intensity at specific wavelengths corresponding to emission lines of vapor-phase species was then compared to the simulated emission intensity at the same wavelength, in a approach similar to the one proposed by Badiola *et al.* [3].

Aluminum flame temperature measurements are interpreted in the context of a change in the flame structure. The largest particles were observed to burn at temperatures close to the alumina vaporization-dissociation temperature and much higher than the aluminum boiling point, suggesting a detached, diffusion-controlled vapor-phase flame, as has been observed for larger particles [17] . As particle size decreases, the flame approaches the particle surface and temperature becomes close to the aluminum boiling point. This is usually interpreted as an indicator that heterogeneous surface reactions are dominant [1] or at least comparable [2] to the vapor phase reaction.

However, no significant reduction in molecular AlO (a vapor phase intermediate) emission was observed, suggesting that heterogeneous kinetic rates may not control the combustion mechanism for aluminum particles as fine as 7 μm in air. SEM imaging of the combustion products has also shown that they consist mainly of an agglomerate of fine particles whose diameter is about 200 nm. These fine particles are coherent with a vapor-phase reaction, in which the alumina formed condensates into nanometric droplets.

5 Conclusion

Experiments of different aluminum and magnesium powders in a 20-l spherical combustion vessel successfully illustrated the differences in combustion characteristics. Magnesium powder presented the fastest reaction rates. Finer aluminum particles were shown to burn faster and have a higher combustion efficiency than the largest aluminum particles. A semi-empirical correlation for estimating burning velocities of dust flames under standardized 20-l sphere dispersion conditions yielded results that correlated reasonably well with burning velocity values previously reported by other authors, and showed a significant particle size influence on aluminum burning velocity in the size range of 7 μm to 18 μm. Temperature measurements confirm a reduction in aluminum dust-air flame temperature for finer particles, indicating that the reaction zone has moved closer to the particle surface. The molecular AlO emissions detected in this work suggest that a vapor phase flame is present for mean particle diameters as fine as 7 μm. Presence of gaseous MgO during magnesium combustion indicates a detached vapor-phase reaction.

Magnesium and aluminum powders are potential candidates for important practical applications, such as SRM propellants. In this context, standardized CVE experiments, despite of its restrictions and drawbacks, might be able to supply coherent combustion trends that will help quantifying the most important combustion characteristics for each specific practical application.

References

[1] T. Bazyn, H. Krier, and N. Glumac, "Evidence for the transition from the diffusion-limit in aluminum particle combustion," *Proceedings of the Combustion Institute*, vol. 31, pp. 2021–2028, Jan. 2007.

[2] C. Badiola, R. J. Gill, and E. L. Dreizin, "Combustion characteristics of micron-sized aluminum particles in oxygenated environments," *Combustion and Flame*, vol. 158, pp. 2064–2070, Oct. 2011.

[3] C. Badiola and E. L. Dreizin, "On Weak Effect of Particle Size on Its Burn Time for Micron-Sized Aluminum Powders," *Combustion Science and Technology*, vol. 184, pp. 1993–2007, Dec. 2012.

[4] P. R. Santhanam, V. K. Hoffmann, M. a. Trunov, and E. L. Dreizin, "Characteristics of Aluminum Combustion Obtained from Constant-Volume Explosion Experiments," *Combustion Science and Technology*, vol. 182, pp. 904–921, June 2010.

[5] R. Lomba, S. Bernard, F. Halter, C. Chauveau, C. Mounaım-Rousselle, P. Gillard, T. Tahtouh, and O. Guézet, "Experimental characterization of combustion regimes for micron-sized aluminum powders," in *53rd AIAA Aerospace Sciences Meeting and Exhibit*, 2015.

[6] A. Dahoe, R. Cant, and B. Scarlett, "On the decay of turbulence in the 20-liter explosion sphere," *Flow, turbulence and combustion*, vol. 67, pp. 159–184, 2001.

[7] O. Kalejaiye, P. R. Amyotte, M. J. Pegg, and K. L. Cashdollar, "Effectiveness of dust dispersion in the 20-L Siwek chamber," *Journal of Loss Prevention in the Process Industries*, vol. 23, no. 1, pp. 46–59, 2010.

[8] V. D. Sarli, P. Russo, R. Sanchirico, and A. D. Benedetto, "CFD simulations of dust dispersion in the 20 L vessel : Effect of nominal dust concentration," *Journal of Loss Prevention in the Process Industries*, vol. 27, pp. 8–12, 2014.

[9] D. Bradley and A. Mitcheson, "Mathematical solutions for explosions in spherical vessels," *Combustion and Flame*, vol. 26, pp. 201–217, Feb. 1976.

[10] M. Silvestrini, B. Genova, and F. J. L. Trujillo, "Correlations for flame speed and explosion overpressure of dust clouds inside industrial enclosures," *Journal of Loss Prevention in the Process Industries*, vol. 21, pp. 374–392, 2008.

[11] H. M. Cassel, *Some fundamental aspects of dust flames*, vol. 6551. US Department of the Interior, Bureau of Mines, 1964.

[12] D. R. Ballal, "Flame Propagation Through Dust Clouds of Carbon, Coal, Aluminium and Magnesium in an Environment of Zero Gravity," *Proceedings of the Royal Society of London. A. Mathematical and Physical Sciences*, vol. 385, no. 1788, pp. 21–51, 1983.

[13] S. Goroshin, I. Fomenko, and J. Lee, "Burning velocities in fuel-rich aluminum dust clouds," *Symposium (International) on Combustion*, vol. 26, pp. 1961–1967, Jan. 1996.

[14] L. V. Boichuk, V. G. Shevchuk, and A. I. Shvets, "Flame Propagation in Two-Component Aluminum – Boron Gas Suspensions," vol. 38, no. 6, pp. 651–654, 2002.

[15] Y. Shoshin and E. L. Dreizin, "Laminar Lifted Flame Speed Measurements for Aerosols of Metals and Mechanical Alloys," *AIAA JOURNAL*, vol. 42, no. 7, pp. 1416–1426, 2004.

[16] G. Risha, Y. Huang, R. Yetter, and V. Yang, "Experimental Investigation of Aluminum Particle Dust Cloud Combustion," in *43rd AIAA Aerospace Sciences Meeting and Exhibit*, American Institute of Aeronautics and Astronautics, 2005.

[17] E. Dreizin, "Experimental study of stages in aluminium particle combustion in air," *Combustion and Flame*, vol. 2180, no. 95, 1996.